UILU-ENG 84-3610

Report No. 110

A STUDY OF THE MECHANISM OF LASER CLADDING PROCESSES

by

J. Mazumder and L. J. Li*
Department of Mechanical and Industrial Engineering, UIUC
*Visiting Scholar from Hunan University
Hunan, People's Republic of China

A Report of the
MATERIALS ENGINEERING - MECHANICAL BEHAVIOR
College of Engineering, University of Illinois at Urbana-Champaign
July 1984

A STUDY OF THE MECHANISM OF LASER CLADDING PROCESSES

L. J. Li* and J. Mazumder
Department of Mechanical and Industrial Engineering
1206 West Green Street
University of Illinois at Urbana-Champaign
Urbana, IL 61801

Summary

The mechanism of two types of laser cladding processes, one with preplaced powder on the substrate and the other with pneumatically delivered powder at the laser beam interaction zone, is discussed. Energy requirement for both the processes are analyzed using a three-dimensional numerical heat-transfer model. Theoretical predictions are in agreement with experimental data. The ways of making a laser cladding process more energy effective are demonstrated.

*Visiting scholar from Hunan University, Hunan, People's Republic of China.

1. INTRODUCTION

Laser cladding by powder fusion has been studied in laboratories since 1974 [1]. Recently Rolls Royce has introduced this technique for hardfacing turbine blades of aircraft engines [2]. This is a technique where, under controlled conditions, a laser beam melts a very thin surface layer of the workpiece which mixes with the liquid cladding to form metallurgical bonding. The potential for producing novel materials by this process are numerous because of the almost infinite material combinations which can be used for the coating.

The Laser cladding process exhibits many advantages over alternative methods such as plasma spraying and arc welding. These advantages include a reduction in dilution, a reduction in waste due to thermal distortion (very little energy is absorbed by the substrate in comparison with the two mentioned alternatives), a reduction in deposit porosity and a reduction in post cladding machining costs because the material can be more accurately placed. This process also produces good metallurgical bond. Moderately high quenching rate inherent in this process offers the possibilities of producing novel microstructure. This process has been studied systematically by several researchers [3-6] in the past few years.

Belmondo and Castagna [3] made a special Molybdenum base alloy wear-resistant coating on cast iron and other substrates by laser cladding process. They demonstrated that surface layers having complex microstructures with good tribological performance and strong bonds to the base material can be obtained using this process. In their experiment, a chosen mixture of powders for cladding was amalgamated with binders to form a paste which was spread over the surface of the substrate. A 12 kW continuous wave CO_2 laser was used with two high frequency vibrating mirrors to form a 8 mm x 8 mm laser beam. Their

data showed that optimum results were obtained for experiments carried out within the specific energy range of 100-150 J/mm^2. Steen and Courtney [4] established operating conditions for laser cladding of Stellite 12 on Nimonic 75 (1.18 mm thick) sheet. A pile of powder was leveled on the substrate before cladding. They used a 2 KW continuous wave CO_2 laser with defocused Gaussian beam. They reached a conclusion from experimental data that to achieve wetting of the Nimonic 75 sheet by Stellite 12, the specific energy must exceed about 23 J/mm^2 for 0.5 mm initial powder thickness and 27 J/mm^2 for 1.0 mm powder thickness. The relationships between beam power, traverse speed, cladding track width, height and dilution were also investigated experimentally.

It is difficult to clad substrate of irregular shape by preplacing a powder layer on the substrate because of the difficulty of maintaining a uniform layer at the desired sight. Weerasinghe and Steen [5] studied another powder delivery method, where the powdered clad material is directly delivered into the laser substrate interaction region, which has more flexibility and versatility in production. They studied the effect of the process parameters on the quality of the cladding layer and pointed out that "the powder continuously impinging on the melt pool appear to give enhanced energy absorption," but they could not explain it from their main experimental study. It was also demonstrated that the use of a reflective shroud and shot blasted specimens can save laser energy. Powell and Steen [6] used ultrasonic vibration of the substrate while laser cladding which appears to reduce both the thermal stress and the porosity.

All these investigations have demonstrated the feasibility of the process and carried out parametric studies, but the results from different experimental condition, for example, the most important characteristic value (the specific energy) are quite different and have no general meaning.

In order to better understand the laser cladding process, more work is needed in studying its mechanism. A laser cladding process by powder fusion is mainly a heat transfer controlled process. Laser beam heats and melts the powder and the heat transfers to the substrate until the melted powder layer gets to wet the substrate and bonds with it after solidification. An optimum laser cladding process requires both the clad layer and the substrate to maintain their composition with minimum dilution except the small boundary layer. Regarding the mechanism of laser cladding process, the kernel problem is to establish a heat transfer model of the process which is going to be discussed in this paper.

In order to obtain high cooling rate and thus fine microstructure during laser cladding, the specific energy input for the process should be as low as possible. High specific energy input leads to grain coarsening, dilution of clad layer and distortion. Low specific energy input will also make this process more economical and competitive to other alternative methods. This paper analyzes the specific energy input using heat transfer theory for laser cladding processes with preplaced powder and pneumatically delivered powder at the interaction zone. The effects of the specific energy input on dendrite arm spacing and bead shape are also discussed.

2. HEAT TRANSFER MODEL

Laser cladding processes can be divided into two groups as follows:

a. Powder is preplaced on the substrate before the interaction with the laser beam. In this group, there are different powder supply methods: leveling a layer of powder on the substrate or delivering the powder straight ahead of the laser beam.

b. Powder is delivered directly at the laser beam interaction region.

2.1 The Heat Transfer Model of the Process with Preplaced Powder

As the substrate is covered with a powder layer, the laser beam impacts the powder layer first. As the powder layer has low thermal conductivity, the heat flux from the powder layer to the substrate before the powder layer is melted can be neglected. After the powder is melted, the laser beam heats the substrate through the melted powder layer. In this way, the whole laser cladding process can be divided into two successive steps: powder melting, and substrate heating.

It was found that a parameter called specific energy E is useful in characterizing a laser cladding process [3,4] $E = P/bV$, where P is the power of the laser beam, V is the speed of the relative movement between the beam and the substrate. b is the beam width along the direction perpendicular to the movement. It is clear that the specific energy means the energy distributed over a unit area swept by the laser beam.

The specific energy can be separated into two parts correspondingly:

$$E = E_1 + E_2 \qquad (1)$$

where

E_1 = specified energy required for melting powder

E_2 = specified energy needed to heat the substrate

As powder layer has volume absorption of laser beam with high absorptivity, the powder melting step can be accomplished with high absorptivity ϕ_1. Assuming M to be the energy needed for melting one unit cubic cladding metal from room temperature, d be the thickness of the solid cladding layer, we have

$$E_1 = \frac{1}{\phi_1} Md. \qquad (2)$$

E_2 is the specific energy needed in the substrate heating step. If the melting point of the base element of the cladding alloy is much higher than that of the substrate, for example, cladding a molybdenum alloy on cast iron [3], the surface temperature of the substrate must reach the melting point of the molybdenum and a melted layer must be formed in the substrate. In this case, substantial dilution is unavoidable, and since the solidification front finishes at the interface between the clad layer and the substrate shrinkage cavities and porosity occur at or near the interface. For sound cladding the solidification front should finish at the surface [5]. From this point of view this kind of material combination should be avoided except some special cases such as described in Ref. [3] where porosity is needed for lubricant retainment. If the melting point of the base element of the cladding alloy is near that of the substrate, such as our cases of cladding a nickel base alloy or stellite on a mild steel or cladding a stainless steel on a mild steel, the cladding layer can be bonded to the substrate as soon as the thin surface

layer of the substrate is melted with minimum energy consumption and dilution. In this case, an approximate theoretical solution of heat conduction can be obtained and this is useful in showing the relationship of the parameters.

A square beam of 2h x 2h is assumed with uniform power density q and traverse velocity V. At the center section along the moving direction, the heat conduction situation is near that of a light band of 2h in width and infinite in length.

Let h_0 be the part of the light band width consumed in melting the powder layer. 2h' (= 2h - ho) is the part of light band width used in heating the substrate. Considering the temperature at the rear of the light band to be the maximum, the minimum heat flux needed to melt the surface of a semi-infinite substrate is [7]

$$q_0 = \frac{\pi K V T_m}{-2\alpha I(-2L')}$$

T_m denotes melting point of the substrate. K denotes the thermal conductivity and α the thermal diffusivity of the substrate.

$$L' = \frac{Vh'}{2\alpha}$$

$$I(x) = \int_0^x e^{-u} K_0(|u|)\, du$$

$K_0(x)$ is the modified Bessel function of the second kind of order zero. The minimum specific heat energy needed to melt the substrate surface is:

$$R = \frac{q_0\, 2h'}{V} = \frac{\pi\rho C\, h' T_m}{-I(-2L')}. \qquad (3)$$

ρ denotes the density and C the specific heat of the substrate, respectively. The minimum specific beam energy needed for heating the substrate is

$$E_2 = \frac{1}{\phi_2} R \tag{4}$$

where ϕ_2 is the absorptivity of the melted cladding alloy.

It can be seen from the above formulii that the smaller the h', K, ρ, C and the larger the V, the lower the specific energy. This means in order to get higher energy efficiency, a smaller light spot, a substrate with low thermal conductivity, density, and specific heat, and a higher moving speed are needed. If the speed V is high, a larger power density q_0 is needed.

Equation (1) can be written again as following:

$$E = \frac{Md}{\phi_1} + \frac{R}{\phi_2}. \tag{5}$$

Equation (5) can be simplified for quantitative calculations if the thickness of the powder layer is small. Let us consider a typical cladding alloy, Stellite No. 6 powder. When the thickness of the powder layer is as thin as 0.5 mm, the equivalent solid layer d $\approx$ 0.27 mm. The energy needed for melting one unit cubic volume of Stellite from room temperature is $M \approx 10$ J/mm^3. Assuming $\phi_1 = 0.54$, we have

$$E_1 = \frac{Md}{\phi_1} = 5 \text{ J/mm}^2.$$

As we can see later, the total specific energy E is more than 40 J/mm^2. As a first approximation, E_1, the specific energy for melting the powder layer, can be neglected in calculation of the total specific energy. We have

$$E \approx \frac{R}{\phi_2} \tag{6}$$

R can be calculated numerically by a three-dimensional heat transfer model.

2.2 The Characteristic of the Process with Powder Delivered at the Laser Material Interaction Zone

In order to make a laser cladding process more efficient, a high surface absorptivity of laser beam is required. It is well known that melted metal surfaces have higher absorptivities than metal surfaces at room temperature and metal powders with correct size have even higher absorptivities for 10.6 μm laser beam.

As discussed above, in the first process the advantage of the high absorptivity of the powder layer is limited to initial part of the process when a molten alloy layer is formed on the substrate. The rest of the laser cladding process takes place at relatively lower absorptivity of the molten alloy layer. If the powder is not already laid on the substrate before it is impacted by the laser beam, but is pneumatically delivered to the laser beam interaction region, the situation will change. Under certain circumstances, the powder can adhere on the interaction region and the whole interaction region is covered with a melting powder layer which has higher absorptivity to the laser beam. In this way, a more energy efficient laser cladding process is expected. The specific energy of the second process can be expressed as follows:

$$E = \frac{1}{\phi_3} (Md + R)$$

where ϕ_3 is the absorptivity of melting powder layer to the laser beam which is higher than that of a melted alloy layer ϕ_2. If, we have

$$\phi_2 < \phi_3$$

the specific energy of the second process can be smaller than the first one.

3. EXPERIMENTAL PROCEDURE

The laser used for this work was an AVCO 10 KW CW CO_2 laser with an annular beam (TEM^*_{01}) output. In order to get a larger and more uniform cladding layer, a rectangular beam is necessary. Therefore, an integrating mirror was used to focus the output beam to a 1/2 in. x 1/2 in. area with uniform power density. As the power density of this beam was too low, a concave spherical mirror was used to reform it to a 6 mm x 6 mm light spot. The optical system is shown in Fig. 1.

The time characteristic of the output of the laser used in these experiments was as shown in Fig. 2. At the time interval T_1, power output increased linearly with time. In this way, the variation of the cladding processes under different power density could be revealed in one run. At the time interval T_3, the output of the laser beam suddenly stopped in 0.1 s, so that the situation of the interaction of the laser beam with the powder and the substrate could be frozen to some extent.

Two kinds of powders were used, Stellite No. 6 powder and a special nickel base alloy powder (80% Ni, 12% Cr, 6% Al, 2% Hf), with different powder handling methods.

Stellite No. 6 powder was leveled on 9 mm thick mild steel or 6 mm thick stainless steel 304 plates before cladding. The thicknesses of the layers were 0.5, 1.0, 1.5 mm, respectively. No attempt was made to pack down the powder layer. By means of weighing powder covered samples, it was determined that the powder density of Stellite No. 6 was 54 percent of the solid density. After cladding, a transparent lacquer was used to "freeze" the solid-liquid interface in the powder for further examination.

Nickel base alloy powder was pneumatically delivered from the screw powder dispenser as shown in Fig. 3.

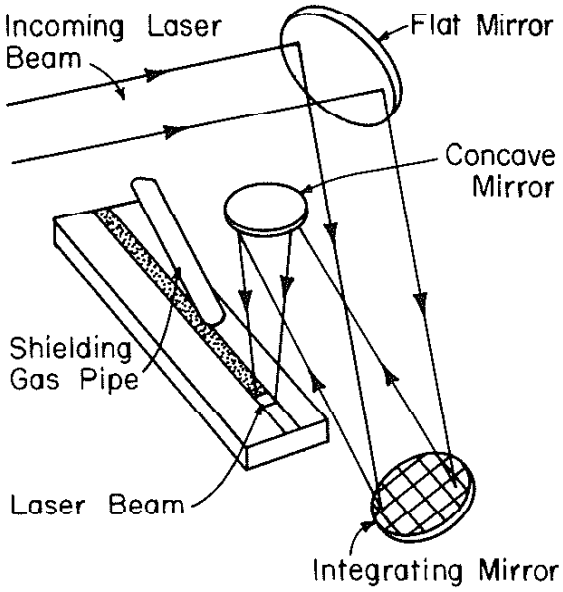

Figure 1 The Optical System

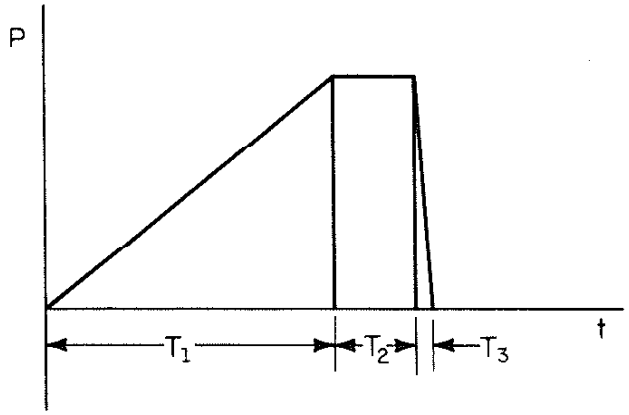

Figure 2 The Time Characteristics of Laser Output

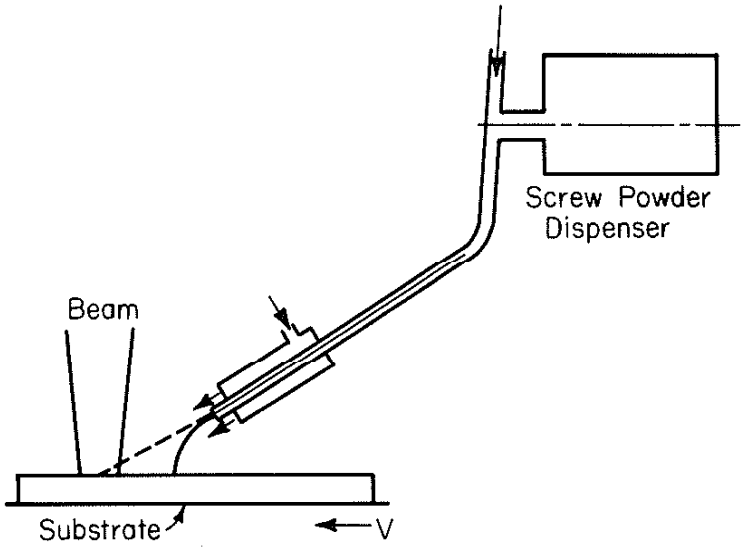

Figure 3 Pneumatic Powder Delivery System
(The powder can be supplied either at the interaction region (solid line) or ahead of the beam by changing the gas flow through the inner pipe)

The powder feed rate can be controlled by changing the turning speed of the screw. The powder feed rate used in these experiments was 7.8 g/min.

As shown in Fig. 3, there was a concentric two-pipe nozzle. The helium gas from the outer pipe was the shielding gas. A variable amount of helium gas helped to blow the powder from the 3 mm diameter inner pipe. The powder supply situation could be changed from delivering the powder in front of the laser beam (solid line in Fig. 3) to shooting the powder to the laser beam interaction region with different gas and powder speed (dashed line) by changing the flow of the gas through the inner pipe. This offered a convenient way to compare the laser cladding process of the first group to that of the second one. The substrate for cladding nickel base alloy was mild steel plates.

The diameter of the Stellite No. 6 powder was about 100 micron and that of the nickel powder was 5 micron. In order to shoot and maintain the powder at the laser beam interaction region, the powder should be fine. That is why the coarse Stellite No. 6 powder was not used with the pneumatic delivery method.

4. EXPERIMENTAL RESULTS AND DISCUSSION

The heat transfer model was verified by the experimental results. Figure 4 shows the sections of specimens along their traverse direction. Before cladding, Stellite No. 6 powder was leveled on a mild steel plate with different powder layer thicknesses d' of 0.5, 1.0, 1.5 mm, respectively. When cladding, the substrate with the powder layer moved from right to left with a traverse speed of 10 mm/s under the stationary laser beam whose ultimate output was 4 KW and suddenly stopped in 0.1 s.

From Fig. 4, we can distinguish the successive two steps of the whole cladding process. The powder layer has an oblique top contour corresponding to the gradual melting of the powder layer when it moved in to the laser beam. The horizontal length of the oblique part is the part of the beam width consumed in melting the powder layer which we expressed by h_0. The melted alloy solidified on the substrate region where it achieved wetting. The end of the cladded layer also has an inclined top contour, since the melted cladding material under the laser beam is swept backwards toward the solidification zone by the surface tension gradient generated by the temperature gradient between the impact region of the laser beam and the trailing solidification front [8].

The minimum stopping time of the laser is 0.1 s which is still too long to preserve the cladding situation exactly, because in 0.1 s, the specimen moved 1 mm. In spite of the stopping delay of the laser and the aberration of the optical system, it still can be seen that the power needed for melting the powder layer becomes smaller when the thickness of the powder layer decreases. When the powder layer is as thin as 0.5 mm, h_0 is only a small part of the light spot dimension of 6 mm. The specific energy needed for melting the powder layer is only a small part of the total specific energy of

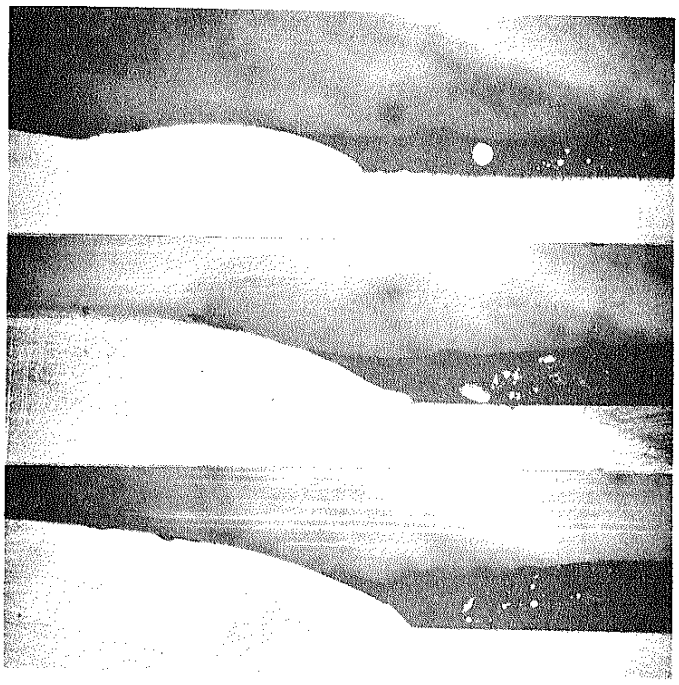

Figure 4 Sections of Specimens along their Traverse Direction at the End of Runs with "Frozen" Unmelted Powder (When cladding, the substrate with the powder layer (thickness = d') moved from right to left with a traverse speed of 10 mm/s under the stationary laser beam with a power characteristic as shown in Fig. 2, reaching up to a maximum power of 4 kW; the ramp down time for the power was 0.1 s)

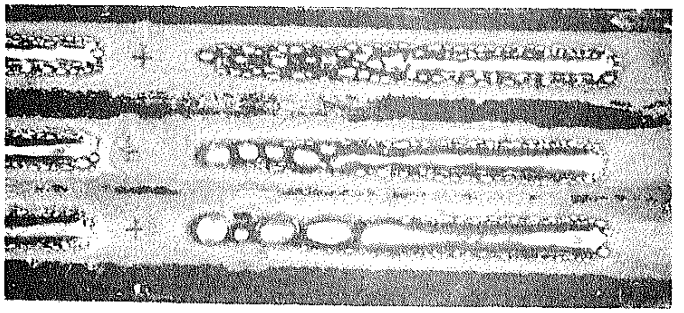

Figure 5 Composite Macrograph showing Three Stellite No. 6 Cladding Specimens with Powder Layer Thickness d' of 0.5, 1.0, 1.5, mm, respectively (The output of the laser beam was as shown in Fig. 2 which began impacting the powder layer at the cross marks on the left, the ultimate output of the laser was 4 kW)

the cladding process and can be neglected. In this case, from the point of view of heat conduction, the role of the powder layer seems only to offer a melted alloy layer on the substrate with higher beam absorptivity as it melts immediately as soon as the laser beam impacts on it.

Figure 5 is a composite macrograph showing three Stellite No. 6 cladding specimens with powder layer thickness d' of 0.5, 1.0, 1.5 mm, respectively. The output of the laser beam was as shown on Fig. 2 which began impacting the powder layer at the cross marks on the left. The ultimate output of the laser was 4 KW. At very low power density, the powder did not melt. As the power density went up, the surface layer of the powder began melting and then the whole powder layer melted to form drops on the substrate when it is solidified. At lower power density, the drops did not adhere to the substrate, but at high power density, the drops achieved wetting of the substrate. Continuous cladding bead was formed after certain power density was reached which corresponded to minimum specific energy needed for laser cladding.

The average values of minimum specific energy for reproducable experimental results for laser cladding with different powder thickness, specimen traverse speed and substrate materials are shown on Fig. 6.

As analyzed before, minimum specific energy decreases as traverse speed increases. For stainless steel substrate, minimum specific energy is much less than that for mild steel. This is because of the lower thermal conductivity and thickness (6 mm) of the stainless steel compared to 9 mm thick mild steel plate.

For comparison, Steen got similar experimental results where to achieve wetting of the 1.18 mm thick Nimonic 75 sheet by the Stellite No. 12, the specific energy must exceed about 23 J/mm^2 for 0.5 mm initial powder thickness

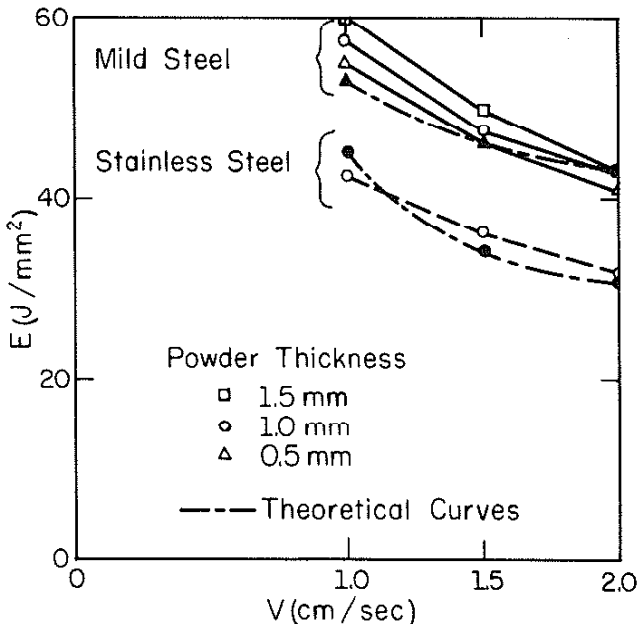

Figure 6 Minimum Specific Energy versus Traverse Speed with Different Powder Thicknesses and Substrate Materials

[4]. Nimonic has low thermal conductivity and the substrate sheet used in his experiment was thin enough to reach its melting point. In cladding a molybdenum alloy on a cast iron substrate, Belmondo and Castagna obtained experimental results where the minimum specific energy was 100 J/mm^2 [3] which is much higher than the value we got. The reason is that the melting point of molybdenum is as high as 2610°C which is much higher than that of cobalt of 1473°C.

From Fig. 6, we can see that the powder thickness does not have much influence on the minimum specific energy. Comparing the two cases of 0.5 and 1.5 mm powder thickness, $\Delta d = (1.5 - 0.5) \times 0.54 = 0.54$ mm

$$\Delta E_1 = \frac{M \Delta d}{\phi_1} = \frac{5.4}{\phi_1} \text{ J/mm}^2.$$

ΔE_1 and ΔE should be more than 5.4 J/mm^2, but the experimental results are less than 5.4J/mm^2. We believe the reason for this phenomenon is that when the powder layer is thin, the melted layer is easy to be broken into separate droplets under surface tension action, and when the powder layer is thick, the melted layer attempts to concentrate to the symmetric line to form a line of big drops when it is solidified as can be seen from Fig. 5. The concentrated, overheated, melted alloy heats the substrate and helps to achieve wetting of the center part of the substrate. This effect compensates for the more energy consumption for melting the thicker powder layer.

Equation (6) offered a way of calculating the minimum specific energy E, but quantitative comparison between the theory and the experimental results need numerical method to calculate specific energy R and E more accurately. Chande and Mazumder developed a three-dimensional heat transfer model for laser materials processing using finite difference numerical techniques which

accounted for variable thermal properties [9]. Using this model with a uniform square beam, we can calculate the power needed for the laser beam melting of the surface of the substrate through the cladding alloy layer that is the beam power when the maximum temperature of the substrate surface reaches its melting point.

Among all the variables included in the calculation, there is only one item we do not know exactly, that is the absorptivity of the melted stellite layer. But we can deduce it from comparing the calculation with the experimental data. The calculated results with an absorptivity of the melted Stellite layer of ϕ_2= 0.37 are also plotted on Fig. 6. The curves for mild steel and stainless steel substrates are in a close agreement with the experimental results. As mentioned before, in the calculation, the energy needed for melting the thin powder layer is neglected.

From Fig. 5 we can see that as the power density increases, the width of the cladding bead increases but the height of the bead decreases. Figure 7 shows two cross sections from the same run while the powers were 2.8 KW and 3.4 KW, respectively. During that run, the light beam spot was 6 x 6 mm^2 and the thickness of the stellite powder layer was 1 mm. The areas of these two beads are the same, that is the melted area of 6 mm wide and 1 mm thick powder layer.

Under the action of a moving square beam with uniform energy distribution, the temperature of the substrate part under the center part of the beam is higher than that of the side parts. As the power density increases, the width of the substrate region whose temperature is above the melting point and on which the melted alloy achieves wetting becomes larger and, in this way, the bead becomes wider. Up until now, we can see that the width of the cladding bead is somehow less than the width of the melted powder

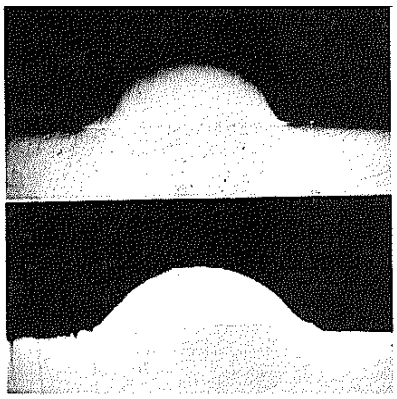

Figure 7 Two Cross Sections of Stellite Clad Beads from the Same Run while the Powers were 2.8 kW and 3.4 kW, respectively (The powder layer of 1.0 mm thick was preplaced on stainless steel plate, the beam spot was 6 x 6 mm^2., the traverse speed was 10 mm/s)

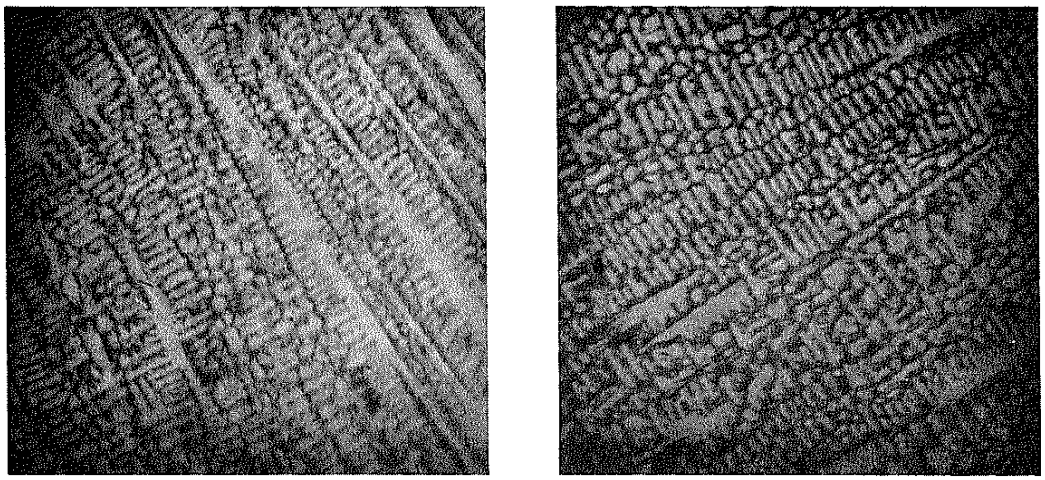

Figure 8 Two SEM Micrographs at 500 X Magnification for the Stellite Clad Beads for the Same Run as that of Fig. 7 where the Powers were 2.8 kW and 4.0 kW, Respectively

layer. Note, the specific energy E means the energy distributed to unit area swept under the laser beam or unit area of melted powder layer but not the unit area of cladded layer.

Figure 8 shows two micrographs at 500 x magnification for the beads for the same run as that of Fig. 7 where the powers were 2.8 KW and 4.0 KW, respectively. The relationship between the dendrite arm spacing and the incident laser power are shown in Fig. 9. Because of the relatively high cooling rate, the grain sizes are small. Specific energy decreases with the decrease of power leading to the higher cooling rate and smaller grain size. From this point of view, the specific energy should not be too much higher than that needed for getting wet.

To demonstrate the difference of the two processes mentioned before, an experiment was conducted. Nickel base alloy was supplied on mild steel plates by pneumatic delivery as shown in Fig. 3. The experimental results of the relationship between minimum specific energy and gas flow (gas speed) are summarized on Fig. 10. 0.25 SCFH gas flow corresponds to delivering a powder layer in front of the beam and the other gas flows correspond to shooting the powder to the laser beam interaction region with different speeds.

From Fig. 10 we can see that shooting the powder into the interaction region can lead to lower specific energy than delivering a powder layer on the substrate before laser beam, and there is an optimal gas flow at which the specific energy is the lowest. In our case, that is 3 SCFH with a gas velocity of 3.3 m/sec.

Figure 11 is a cross section of a clad bead where the gas flow was 3 SCFH, the laser power was 4 KW, the tranverse speed was 10 mm/sec and the specific energy was 66.7 J/mm^2. When the cladding process was finished, there is a thin powder layer covering the clad layer. Figure 12 is a SEM micrograph

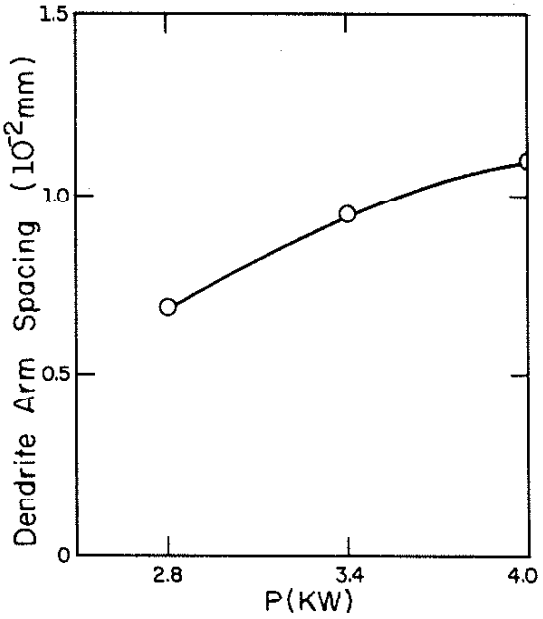

Figure 9 Variation of Dendrite Arm Spacing with Laser Power

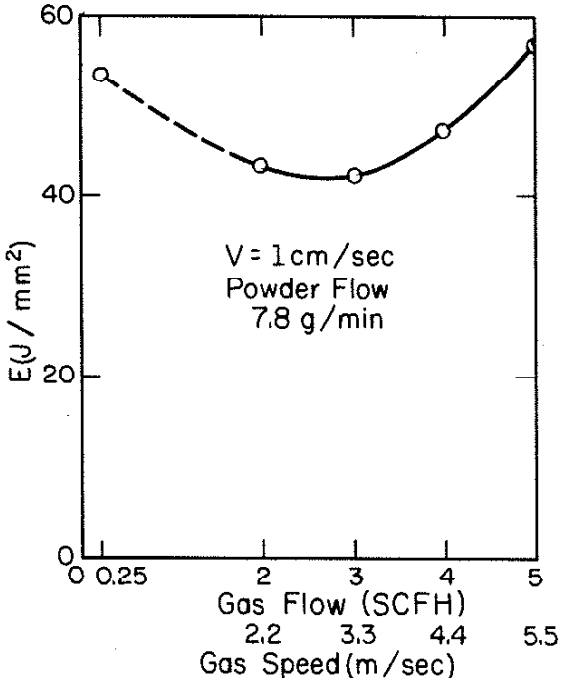

Figure 10 Variation of Minimum Specific Energy with Gas Flow and Gas Speed (0.25 SCFH Gas Flow Corresponds to Delivering a Powder Layer in Front of the Beam and the Other Gas Flows Correspond to Shooting the Powder to the Laser Beam Interaction Region with Different Speeds)

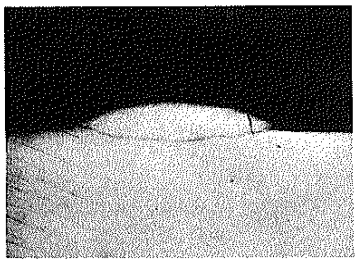

Figure 11 Cross Section of a Clad Bead with Pneumatically Delivered Powder of Nickel Base Alloy at the Laser Beam Interaction Region (The gas flow was 3 SCFH, the laser power was 4 kW, the traverse speed was 10 mm/s, the substrate was mild steel plate)

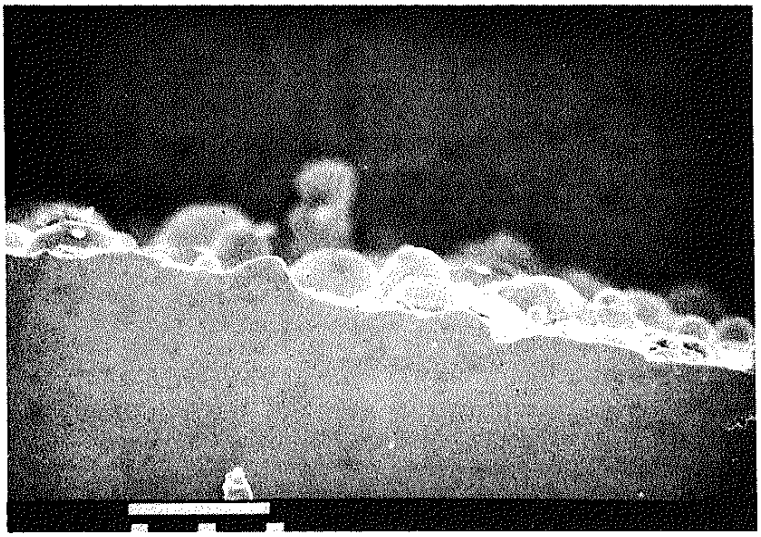

Figure 12 SEM Micrograph of Bead Surface shown in Fig. 11

of the surface of the bead shown in Fig. 11. A layer of spheres of clad material with a diameter of about 50 micron covers the surface of the clad layer. These spheres are not the 5 microns diameter powder, but the melted and resolidified powder which passed through the laser beam. This is a demonstration that powder can be melted when it passes through the laser beam and the melting powder can adhere to the interaction region, but it also shows that some of the powder went through the laser beam and was lost.

It is interesting to note that the experimental result of nickel base alloy with 0.25 SCFH gas flow is comparable with that of Stellite No. 6. The specific energy of the former is 53.5 J/mm^2, and the specific energy of the latter with 0.5 mm thick powder layer and the same traverse speed (1 cm/sec.) is 54.9 J/mm^2. The powder supply methods of the two experiments were different, but they all belong to the same group that the powder is already laid on the substrate before it is impacted by the laser beam and the cladding mechanisms should be the same. The substrate used in both experiments were the same. This verified the hypothesis presented before that it is not the powder, but the substrates, their thermo-physical properties and dimensions, that dominate the amount of heat needed for cladding, especially when the powder layers are thin.

5. CONCLUSION

1. Laser cladding processes can be divided into two basic groups: preplaced powder on the substrate before it is impacted by the laser beam and powder is pneumatically delivered to the laser beam interaction region. The mechanisms of two groups are different.
2. If the powder is already laid on the substrate before it is impacted by the laser beam, the whole cladding process consists of two successive steps: powder layer melting and substrate heating through the melted powder layer.
3. If the powder layer is relatively thin, the specific energy needed for powder melting is negligible and the heat conduction of the process can be treated as laser beam incident on the substrate surface with an absorptivity of the melted powder layer.
4. Comparing the results of numerical calculation with the experimental data, it was deduced that the absorptivity of the melted stellite layer to the laser beam is 37 percent. The calculated relationships between minimum specific energy and traverse speed and materials are in close agreement with the experimental data.
5. Powder thickness does not have much influence on the minimum specific energy of laser cladding processes within the experimental parameter range, so the calculation for thin powder layer can be used to estimate the minimum specific energy for thicker powder layer.
6. Analysis and experimental results show that in order to get higher energy efficiency, a smaller light spot, a substrate with low thermal conductivity, density and specific heat, and a higher traverse speed are needed.

7. The area of the cross section of a laser clad bead equals that of the melted powder, but the width of the bead depends on how wide a region the substrate gets wet. Higher the laser power and specific energy, wider and shorter the bead.
8. In order to obtain a fine grain size for the clad layer, the specific energy should not be much higher than the minimum one for getting wet and making bond.
9. If the powder is shot to the laser beam interaction region, under certain circumstances the powder can adhere on the interaction region and the whole region is covered with a melting powder layer which has higher absorptivity to the laser beam. In this way, a more energy efficient laser cladding process is expected. In this experiment, the optimal gas blow velocity for lowest minimum specific energy is 3.3 m/sec.

ACKNOWLEDGEMENTS

The authors express their appreciation to Engineer Jon Culton for his cooperation and help in experimental methods. The cooperation of Mr. Tom Cosale for laser experiments is also appreciated. This work is partially funded by a grant from University of Illinois Materials Processing Consortium. Author L. J. Li would like to acknowledge the financial support from the People's Republic of China.

REFERENCES

1. Seaman, F. D., and D. Gnanamuthu, Metal Progress, Vol. 108, No. 3, p. 67, 1975.

2. McIntyre, M., "Laser Hardfacing of Turbine Blades," Applications of Laser in Materials Processing, E. A. Metzbower (ed.) published by ASM, 1983.

3. Belmondo, A., and M. Castagna, "Wear-Resistant Coatings by Laser Processing," Thin Solid Films, 64, p. 249-256, 1979.

4. Steen, W. M., and C.G.H. Courtney, "Hardfacing of Nimonic 75 Using 2 kW Continuous Wave CO_2 Laser," Metals Technology, p. 232-237, June 1980.

5. Weerasinghe, V. M., and W. M. Steen, "Laser Cladding with Pneumatic Powder Delivery," Application of Laser in Materials Processing, E. A. Metzbower and S. M. Copley (Eds.), ASM, 1983.

6. Powell, J., and W. M. Steen, "Vibro Laser Cladding," pp. 93-104, Lasers in Metallurgy, edited by K. Mukherjee and J. Mazumder, 1981.

7. Jaeger, J. C., "Moving Sources of Heat and the Temperature at Sliding Contacts," Proc. of the Royal Society of New South Wales, 76, 1943.

8. Anthony, T. R., and H. E. Cline, "Surface Rippling Induced by Surface-Tension Gradients during Laser Surface Melting and Alloying," J. of Applied Physics, Vol. 48, No. 9, September 1977.

9. Chande, T., and J. Mazumder, "Heat Flow During CW Laser Materials Processing," PP 165 Lasers in Metallurgy, published by TMS-AIME, K. Mukerjee and J. Mazumder, (Eds.), 1981.